Blockchain-enabled Robust-game Electricity Transaction Model for a Multi-microgrid System Considering Wind Power Uncertainty

Jiayu Wu, *Member*, *CSEE*, Yang Liu, Qiming Yang, and Wenfeng Li

***Abstract*—Considering the uncertainty of wind power generation (WPG) and the specific operation behaviors of trading microgrids, this paper presents a blockchain-enabled robust-game electricity transaction model in a multi-microgrid system (MMS) to obtain optimal bidding-dispatching strategies, and achieve a transparent and decentralized electricity transaction. Combining blockchain technology and a non-cooperative game model, the established MMS electricity transaction architecture provides a complete information game environment for all game microgrids and facilitates the transparent, efficient, orderly, spontaneous management of MMS electricity transactions without the intervention of a third trusted party. Based on the distributed transaction architecture, an MMS robust-game model is presented to achieve the optimal day-ahead bidding-dispatching (DA-BD) strategies, in which the individual microgrid two-stage adjustable robust-game bidding-dispatching (ARG-BD) model characterizes the WPG uncertainty by employing uncertain interval and adjustable robust parameters. The binary expansion method, duality theory, big M method, and column-and-constrain generation algorithm (C&CG) are employed to solve the individual microgrid two-stage ARG-BD model. An alternating robust-game procedure integrating the C&CG algorithm and non-cooperative game model is developed to solve the MMS robust-game model. Case studies demonstrate the transparent and decentralized transaction, economic mutual benefits, and solution robustness of the presented method.**

***Index Terms*—Alternating robust-game procedure, bidding-dispatching model, blockchain technology, individual microgrid robust-game, MMS robust-game model, WPG uncertainty.**

I. Introduction

RENEWABLE energy sources (RES), especially wind power, have been wildly employed in modern power systems to solve the increasingly severe environmental contamination and energy crisis problems [1], [2]. Meanwhile, the microgrid has been well regarded as a remarkable way of accommodating RESs with uncertain output due to the flexible operation and high degree of autonomy features [3]. With the escalation of microgrid numbers and the increasing penetration of wind power generation (WPG), the frequent energy interaction between microgrids and the connected distribution network (DN) aggravates the operation pressure of DN [4]. Interconnected microgrids in the same DN can form a multi-microgrid system (MMS) [4], [5]. Initiating electricity transaction among MMS enables to improve the overall economy [6], promote the consumption of a RES [7] and reduce unnecessary energy interaction with the DN [8]. However, the various trading status of microgrids determined by different energy profiles make electricity transactions more flexible, which complicates the market competition. The complicated competition and interest coupling relationship of microgrids brings huge challenges to achieving the optimal trading strategies [9], [10]. In addition, the uncertainty of WPG significantly impacts the economy and reliability of MMS transactions due to their deterioration in the operation and regulation behaviors of trading microgrids [11], [12]. Therefore, it is necessary to establish an effective electricity transaction model to coordinate the complicated interest coupling relationship of microgrids and cope with the uncertainty of WPG.

Currently, many scholars have launched numerous research focusing on the MMS trading mechanism. Considering the uncertainty of WPG, research [13] constructs a regional MMS-DN trading model to minimize the operation cost of MMS. This model regards MMS as a whole and ignores the complicated competition-cooperation relationship between individual microgrids [14]–[16]. Game theory, which has demonstrated great effectiveness in analyzing the complicated interest interaction relationship, has been gradually introduced into MMS electricity transaction problems [17]–[21]. Under the guidance of DN, the microgrids in research [17] can participate in MMS electricity transactions through the game of electricity bidding prices and bidding amounts to obtain reasonable profits. The non-cooperative leader-followers game model of DN and MMS proposed in research [18] encourages microgrids to participate in distribution market transactions to reduce DN operation costs. However, the microgrids in research [17], [18] are regarded as dispatched units to respond to upper-level incentives or constraints when participating in electricity transactions. For MMS with a high penetration of RES, research [19] proposes an MMS transaction framework by integrating the game-theoretic and hierarchical optimization approach to reduce the dependency on DN and minimize the operation costs, while the impact of RES uncertainty on transaction strategy formulation is ignored. Research [20] pro-

Manuscript received July 3, 2021; revised September 27, 2021; accepted December 4, 2021. Date of online publication September 5, 2022; date of current version December 4, 2024.

J. Y. Wu (corresponding author, email: wujiayu0325@163.com), Y. Liu and Q. M. Yang are with College of Electrical Engineering, Sichuan University, Chengdu 610065, China.

W. F. Li is with State Grid Corporation of China Henan Electric Power Company, Zhengzhou 450000, China.

DOI: 10.17775/CSEEJPES.2021.04830

poses a Stackelberg equilibria-based game model to peruse the interest interaction relationship among MMS and determine the optimal trading strategy of each game microgrid in order to maximize the economic mutual benefits. In research [19], [20], the microgrid independently participates in electricity transactions based on its own interests, which is able to formulate the trading strategy according to different energy profiles. The effectiveness of the above studies is verified, but none of them take into full consideration the uncertainty of RES and the detailed operation and regulation behaviors of MMS with electricity interaction.

The uncertainty of WPG deteriorates the operation and regulation behaviors of the trading microgrids, and further impacts the economy and reliability of MMS transactions [11], [12]. Therefore, the uncertainty of RES can be tackled by a bunch of optimization methods, such as stochastic optimization (SO), deterministic optimization (DO), and robust optimization (RO). Research [22] employs DO to deal with the uncertainty of RES. However, DO has proved that it makes little contributions for dealing with uncertainty [23]. Research [24] applies SO to achieve the optimal pricing strategies of the interconnected microgrids in MMS transactions. Nevertheless, research [25] points out that SO is computationally intensive and highly uncertain probability distribution function dependent. Considering the uncertainty of WPG, research [26] presents a two-stage adaptive RO model for the optimal scheduling of MMS. RO adopts the uncertainty sets to capture the RES uncertainty rather than the precise probability distributions, which greatly reduces the computation complexity and strictly immunizes the RO solution against RES worst-case scenarios. However, research [27], [28] claims that the overly conservative results are likely to be obtained with RO. Compared with the traditional RO method, by introducing an adjustable robust parameter, adjustable robust optimization (ARO) can reach a better balance between the robustness and economy. The key of ARO is to adjust the occurrence of worst-case scenarios. The uncertainty tackling ability of ARO is demonstrated in the two-stage ARO short-term operation framework of microgrids presented in [29].

More complex and diverse microgrid data needs to be processed in MMS transactions due to the uncertainty of RES and increasing scale of MMS [30], [31]. In this case, the traditional centralized transaction mode with the problems of low anti-risk ability, information opacity and low efficiency of information circulation is developing towards a decentralized manner to achieve secure and efficient MMS transactions [32]. As a distributed shared ledger and chained database, blockchain technology with the characteristics of data transparency, decentralization, and high security is an ideal underlying technology for distributed energy trading. Research [33], [34] investigate the adaptability of blockchain technology in the application of distributed energy trading. Based on multi-agent consortium blockchain, research [35] proposes a trading system in DN to achieve distributed and equal transactions between prosumers. Research [36] proposes the blockchain-based operation mechanism, real-time dispatching transaction process and supervision model for a electricity spot market. The above studies indicate that the application of blockchain technology can avoid possible transaction disputes and ensure the security of the trading system. Blockchain technology has gradually been applied in MMS electricity transactions. Research [37] constructs a blockchain-enabled competition game model of MMS transactions. The proposed real-time hybrid game pricing model indicates that the integration of blockchain technology contributes to achieve the economic mutual benefits of supply and demand side, improve the efficiency of the electricity transaction and promote the development of the electricity market [38]. Combining blockchain technology and game-theoretics, research [39] proposes an MMS trading game model to obtain the optimal trading strategies and achieve a transparent transaction. Research [37]–[39] indicates that the application of blockchain technology facilitates the transparent, efficient, orderly and spontaneous management of MMS electricity transactions.

In the above literature, it can be found that the transparent and decentralized MMS electricity transaction frameworks considering WPG uncertainty and complicated interest coupling relationship of microgrids is limited. This paper establishes a blockchain-enabled robust-game electricity transaction model to achieve the transparent and decentralized electricity transaction and acquire the optimal bidding-dispatching strategy. The main results of this paper are as follows:

1) The MMS electricity transaction architecture is established by combining blockchain technology and the non-cooperative game model, providing a complete information game environment for all game microgrids in the trading strategy formulation stage. The smart contracts describing the MMS electricity transaction rules are embedded into the blockchain-enabled transaction platform to achieve the decentralized and trusted transaction in an efficient way.

2) Based on the distributed transaction architecture, an MMS robust-game model is presented which integrates the two-stage ARO model and non-cooperative game model organically to achieve the optimal bidding and dispatching strategies. The first stage of the individual microgrid two-stage adjustable robust-game bidding-dispatching (ARG-BD) model seeks the optimal bidding and dispatching strategy. In the second stage, the worst-case scenario of WPG is regarded as the primary priority and the optimal strategy of bidding and dispatching can be obtained.

3) The binary expansion method and column-and-constraint generation algorithm are introduced as significant tools to deal with the individual microgrid two-stage ARG-BD problem, as well as the duality theory and big M method. The alternating robust-game procedure integrating the C&CG algorithm and non-cooperative game model is developed to solve the MMS robust-game model.

The presented approach is tested on a decentralized electricity trading platform, which is constructed by combining the ethereum client Ganache, Metamask wallet and Remix online compiler. Case studies demonstrate the transparent and decentralized transaction, economic mutual benefits, and solution robustness of the blockchain-enabled robust-game electricity transaction model.

II. MMS Electricity Transaction Architecture Based on Blockchain Technology

The prosumer characteristic of microgrid makes the MMS electricity transaction more flexible, which complicates the market competition. The complicated competition and interest coupling relationship of microgrids brings huge challenges to achieve the optimal trading strategies. Therefore, a non-cooperative game model is employed to handle the conflict of interest and competition relationship between different trading microgrids. The game process of the MMS transaction non-cooperative game model under the traditional centralized transaction management mechanism is shown in Fig. 1. Selling microgrids upload the real-time transaction information to the transaction center, which integrates and publishes the organized transaction information. Each microgrid reformulates the optimal transaction strategy according to the newly published transaction information and its own operation condition, and then uploads the updated transaction information. The optimal Nash equilibrium can be acquired by a repeatedly iterative process [38]. In the traditional centralized transaction management mechanism, the transaction information required to develop the optimal trading strategy can only be searched from the data processed by the transaction center, which leads to poor information transparency [39] and low information circulation efficiency [40]. The transaction center, as the information hub of a MMS transaction, is susceptible to malicious attacks and data manipulation [41]. While blockchain technology facilitates the transparent, efficient, orderly and spontaneous management of MMS electricity transactions without intervention of a third trusted party due to the characteristics of data transparency, decentralization, and high security. It is an ideal underlying technology to support the non-cooperative game model of MMS transaction.

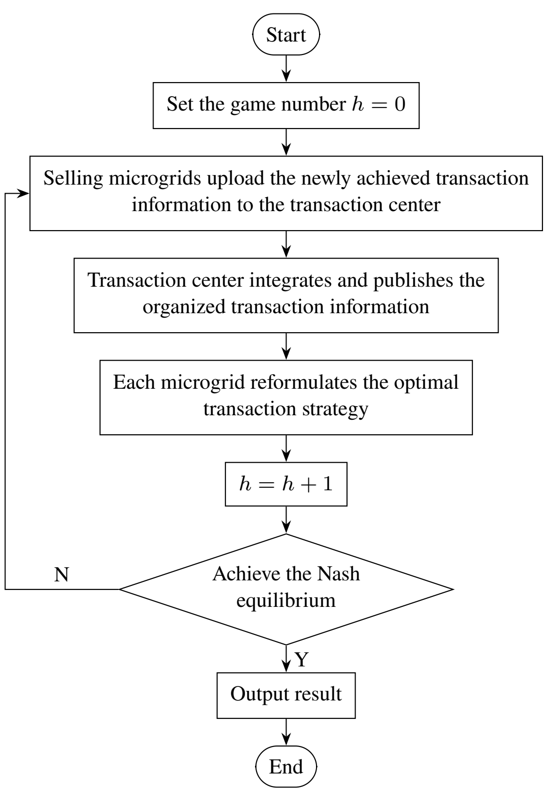

Fig. 1. MMS Game process under the centralized transaction mode.

A. The Combination Between Blockchain Technology and MMS Transaction Procedure

1) Blockchain technology and smart contract

As a distributed shared ledger and chained database, blockchain technology is able to achieve the distributed interaction and collective maintenance of transaction information in a decentralized and trusted manner. All transaction information of MMS is updated synchronously in each microgrid node, which greatly improves the transparency of transaction information. Instead of collecting transaction information through a third trusted party, each microgrid node on the blockchain trading platform can directly obtain the related transaction information, providing a complete information game environment for all game players. The transaction information stored on the blockchain is open to every microgrid node. The account identity information and the operation data of each trading microgrid are highly encrypted, which can only be accessed with the authorization of the data owner, so as to ensure the data security and personal privacy. The adopted consensus algorithm in the blockchain platform can ensure the security and authenticity of the updated transaction information. Blockchain is a chain composed of data blocks, which are arranged in chronological order. These chained-blocks consist of a block header and block data. The specific transaction information including the trading microgrid identity, the electricity trading price, amount and the transaction time are stored in the block data. The block header includes the version number, the uniquely generated hash value and the Merkle tree, which are employed to link the next data block and identify each block. If any of the chained-blocks is removed or manipulated, the uniquely generated hash value will change and the manipulated block cannot be linked to the next block. Blockchain technology is able to provide a decentralized and transparent transaction environment, and ensure the security of transaction information.

The smart contract is an event-driven computerized transaction protocol that contains the predefined transaction rules and terms, and it can be automatically executed in a prescribed manner when the preset response condition is triggered. By embedding the smart contract into the blockchain platform, the decentralized and trusted transaction can be achieved in an efficient way.

2) Classification of blockchain

Blockchain can be divided into the public blockchain and the private blockchain according to the node record authority.

Consortium blockchain is a cluster composed of private blockchains. The blockchain is managed by multiple institutions, and each institution controls one or more nodes. The data can only be read, written and sent by different institutions in the system. The consortium blockchain is essentially a private blockchain.

In a public blockchain, each node has the authority to read and write the data on the chain, and complete decentralization can be achieved. However, the following problems make the public blockchain difficult to adapt to the market environment: (1) The transaction information needs to be transmitted to most of the nodes in the network to achieve transaction consensus. Too many nodes in the public blockchain lead to long communication times and low transaction efficiency. (2) Since the information on the public blockchain is open to every node, the users' privacy cannot be guaranteed. (3) Every node needs to keep all transaction records, which requires huge storage capacity for each node.

In a private blockchain, only a few nodes have the complete authority to read and write blockchain data, and the authority of other nodes is limited. The decrease of the recode nodes leads to the reduction of transaction consensus time and the improvement of transaction efficiency. Since most of the nodes have limited access to the blockchain data, the users' privacy can be guaranteed. The disadvantage is that the status of each node is not equal, which is contrary to the original intention of decentralization. However, comprehensively considering the communication efficiency and storage capacity, private blockchain is more suitable for the market environment than public blockchain.

3) The MMS transaction procedure based on blockchain technology

As shown in Fig. 2., the specific MMS transaction procedure consists of the trading strategy formulation stage and the transaction stage. In the trading strategy formulation stage, selling microgrids employs a non-cooperative game model to obtain the optimal trading strategies. Each game microgrid is connected to a smart meter, through which the transparent information interaction can be achieved on the constructed blockchain platform. The game environment of the MMS transaction non-cooperative game model at this time is a complete information game. In the transaction stage, the Nash equilibrium obtained in the trading strategy formulation stage triggers the preset response condition of the embedded smart contracts, and then the smart contracts describing the predetermined electricity transaction rules are automatically executed. The transaction results are returned to each trading microgrid. The transaction information is synchronously written into the blockchain to ensure the security and transparency of the transaction.

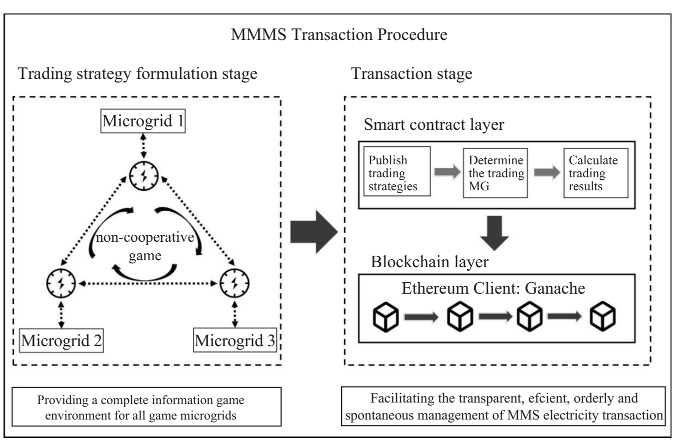

Fig. 2. The MMS transaction procedure based on blockchain technology.

B. Blockchain Based MMS Electricity Transaction Architecture

The specific structure of the MMS electricity transaction architecture combining the blockchain technology and non-cooperative game model is shown in Fig. 3.

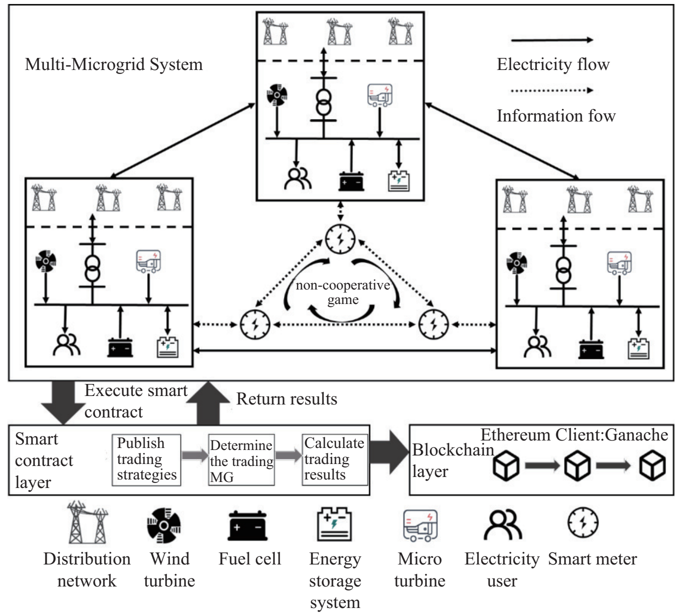

Fig. 3. Architecture of MMS electricity transaction.

Connected with DN, each microgrid consists of a wind turbine, energy storage system (ESS), electricity users and controllable generators. Each microgrid determines the electricity trading price σ_t and amount κ_t at time t according to its own operation conditions and the transaction information of other microgrids. The microgrids that haven't achieved the demand-generation balance after MMS electricity transactions can still trade with DN.

The MMS transaction non-cooperative game model can be described using (1):

$$Z = (G_1, G_2, \cdots, G_n; F_1, F_2, \cdots, F_n) \tag{1}$$

where game players are the microgrids with surplus power; game strategy G_i is the bidding strategy of game player i, containing the electricity bidding price σ_t and amount κ_t; utility function F_i is the total operation cost of game player i; n is the number of game players. The Nash equilibrium of the MMS transaction non-cooperative game model $(G_1^*, G_2^*, \cdots, G_n^*)$ should satisfy $F_i(G_i^*, G_{\mathrm{oi}}^*) \leq F_i(G_i, G_{\mathrm{oi}}^*)$, in which "$oi$" denotes the game players other than the i^{th} game player.

According to the historical bidding strategies of other game players $\{\overline{\sigma}_{\mathrm{oit}}, \overline{\kappa}_{\mathrm{oit}}\}, \forall t \in T$, game microgrid i formulates the corresponding bidding strategy $\{\sigma_{it}, \kappa_{it}\}, \forall t \in T$ and continuously broadcasts it through the smart meter. Other game players receive the broadcast information and reformulate the optimal bidding strategies $\{\sigma_{oit}, \kappa_{oit}\}, \forall t \in T$. The bidding strategies of all game microgrids are reformulated and updated after one round of the game. Game microgrids conduct the next round of games according to the updated bidding strategies. The iterative process is repeated until the optimal

Nash equilibrium $\{\sigma_{1t}^*, \kappa_{1t}^*; \sigma_{2t}^*, \kappa_{2t}^*; \cdots; \sigma_{nt}^*, \kappa_{nt}^*\}, \forall t \in T$ is obtained.

The MMS electricity transaction rules are described in Table I. According to the transaction rules, MMS writes the smart contracts and deploys them to the blockchain-based transaction platform. When the preset response condition is triggered, MMS executes the smart contracts automatically to publish trading strategies, determine trading microgrids and calculate trading results. The transaction information is synchronously written into the blockchain platform.

TABLE I
THE MMS ELECTRICITY TRANSACTION RULES

The MMS transaction rules	
1)	The electricity bidding prices of different game players obtained from the MMS transaction non-cooperative game model are higher than the selling price of DN and lower than the purchase price of DN.
2)	In order to minimize the electricity purchasing cost, the microgrid with a power deficit successively trades with microgrids with surplus power according to the bidding prices from low to high until the demand-generation balance is achieved.
3)	After MMS transactions, the microgrid with power deficit or microgrid with surplus power can still trade with DN to achieve the demand-generation balance.

III. Construction of the MMS Robust-game Model

The presented MMS robust-game model can be described using (2):

$$Z = \begin{cases} G_1 = (\sigma_{1t}, \kappa_{1t}), \forall t \in T \\ F_1 = \min\limits_{x_1, \sigma_1, \kappa_1} \{C_{\mathrm{da}} + \max_{u_1} \min\limits_{y_1} C_{\mathrm{rt}}\} \\ G_2 = (\sigma_{2t}, \kappa_{2t}), \forall t \in T \\ F_2 = \min\limits_{x_2, \sigma_2, \kappa_2} \{C_{\mathrm{da}} + \max_{u_2} \min\limits_{y_2} C_{\mathrm{rt}}\} \\ \quad \cdots \\ G_n = (\sigma_{nt}, \kappa_{nt}), \forall t \in T \\ F_n = \min\limits_{x_n, \sigma_n, \kappa_n} \{C_{\mathrm{da}} + \max_{u_n} \min\limits_{y_n} C_{\mathrm{rt}}\} \end{cases} \tag{2}$$

where Z is the MMS robust-game model; $F_i = \min\limits_{x_i, \sigma_i, \kappa_i} \{C_{\mathrm{da}}(x_i, \sigma_i, \kappa_i) + \max\limits_{u_i} \min\limits_{y_i} C_{\mathrm{rt}}(u_i, y_i)\}$ is the two-stage ARG-BD model of individual microgrid i, which achieves the optimal DA-BD strategy $(x_i, \sigma_i, \kappa_i)$ in each round of the game. σ_t and κ_t are the electricity bidding price and amount; x is the day-ahead economic dispatch strategy; u is the WPG worst-case scenario; y is the corresponding real-time adjustment strategy; C_{da} and C_{rt} are the day-ahead and real-time operation costs.

According to its own operation condition and the historical bidding strategies of other game players $\{\overline{\sigma}_{oit}, \overline{\kappa}_{oit}\}, \forall t \in T$, game microgrid i employs the two-stage ARG-BD model to formulate the optimal DA-BD strategy $\{x_{it}, \sigma_{it}, \kappa_{it}\}, \forall t \in T$, and continuously broadcasts the bidding strategy $\{\sigma_{it}, \kappa_{it}\}$, $\forall t \in T$ through the smart meter. Other game players receive the broadcast information and reformulate the optimal bidding strategies $\{\sigma_{oit}, \kappa_{oit}\}, \forall t \in T$ through the two-stage ARG-BD model. The iterative process is repeated until the optimal Nash equilibrium $\{\sigma_{1t}^*, \kappa_{1t}^*; \sigma_{2t}^*, \kappa_{2t}^*; \cdots; \sigma_{nt}^*, \kappa_{nt}^*\}, \forall t \in T$ is obtained.

The existence of the worst-case scenario is not so frequent during the whole time period. Therefore, to avoid the over-conservative issue, the uncertainty sets and adjustable robust parameters are adopted to illustrate the uncertainty of WPG in the individual microgrid two-stage ARG-BD model, which can be described as follows:

$$\sum_t \left[\frac{P(t) - P^{\mathrm{pre}}(t)}{p_t^+} \rho_t^+ + \frac{P^{\mathrm{pre}}(t) - P(t)}{p_t^-} \rho_t^- \right] \leq \Gamma \tag{3}$$

where Γ is the adjustable robust parameter which is able to coordinate the robustness and economy of the obtained strategies by changing the number of times that the worst-case scenario occurs; P^{pre} is the prediction value; p_t^+ and p_t^- are the fluctuation ranges; ρ_t^+ and ρ_t^- are the 0–1 variables. If the actual value $P(t)$ is larger than the prediction value, $\rho_t^+ = 1$, $\rho_t^- = 0$. Otherwise, $\rho_t^+ = 0$, $\rho_t^- = 1$.

A. Day-ahead Stage of the Two-stage ARG-BD Model

The day-ahead stage of the presented individual microgrid two-stage ARG-BD model can be represented by (4):

$$\begin{cases} \min\limits_{x, \sigma, \kappa} C_{\mathrm{da}}(x, \sigma, \kappa) \\ \text{s.t.} \quad H_{\mathrm{da}}(x, \sigma, \kappa) = 0 \\ \qquad G_{\mathrm{da}}(x, \sigma, \kappa) \leq 0 \end{cases} \tag{4}$$

Based on the known worst-case scenarios of WPG, Microgrid i seeks the optimal bidding strategy (σ, κ) and the day-ahead economic dispatch strategy x to minimize the day-ahead operation costs.

$$\begin{aligned} \min_{x, \sigma, \kappa} C_{\mathrm{da}} &= C_{\mathrm{MT}} + C_{\mathrm{FC}} + C_{\mathrm{Grid}} + C_{\mathrm{MGs}}^{\mathrm{buy}} - C_{\mathrm{MGs}}^{\mathrm{sell}} \\ C_{\mathrm{MT}} &= \sum_t [a_{\mathrm{MT}} \cdot P_{\mathrm{MT}}(t) + b_{\mathrm{MT}}] \cdot \Delta t \\ C_{\mathrm{FC}} &= \sum_t [a_{\mathrm{FC}} \cdot P_{\mathrm{FC}}(t) + b_{\mathrm{FC}}] \cdot \Delta t \\ C_{\mathrm{Grid}} &= \sum_t [\lambda_{\mathrm{Grid}}^{\mathrm{buy}}(t) P_{\mathrm{Grid}}^{\mathrm{buy}}(t) - \lambda_{\mathrm{Grid}}^{\mathrm{sell}}(t) P_{\mathrm{Grid}}^{\mathrm{sell}}(t)] \cdot \Delta t \\ C_{\mathrm{MGs}}^{\mathrm{buy}} &= \sum_t S_{\mathrm{oi}}^{\mathrm{buy}}(t) \cdot [c_{\mathrm{oi}}^{\mathrm{buy}}(t) \cdot P_{\mathrm{oi}}^{\mathrm{buy}}(t)] \cdot \Delta t \\ C_{\mathrm{MGs}}^{\mathrm{sell}} &= \sum_t S_{\mathrm{MGs}}^{\mathrm{sell}}(t) \cdot (\sigma_t \kappa_t) \cdot \Delta t \\ &= \sum_{n=1}^{M} \sum_t S_{\mathrm{MG}s}^{\mathrm{sell}}(t) \cdot (\sigma_{nt} \kappa_{nt}) \cdot \Delta t \end{aligned} \tag{5}$$

where a_{MT}, b_{MT}, a_{FC}, and b_{FC} are the constant coefficients of MT and FC; $P_{\mathrm{MT}}(t)$ and $P_{\mathrm{FC}}(t)$ are the generation outputs of MT and FC; $\lambda_{\mathrm{Grid}}^{\mathrm{buy}}(t)$ and $\lambda_{\mathrm{Grid}}^{\mathrm{sell}}(t)$ are the purchasing and selling prices from DN in day-ahead market; $P_{\mathrm{Grid}}^{\mathrm{buy}}(t)$ and $P_{\mathrm{Grid}}^{\mathrm{sell}}(t)$ are the purchased and sold electricity of the microgrid; $S_{\mathrm{oi}}^{\mathrm{buy}}(t)$, $c_{\mathrm{oi}}^{\mathrm{buy}}(t)$ and $P_{\mathrm{oi}}^{\mathrm{buy}}(t)$ are the electricity purchasing state, price and amount of microgrid i from other microgrids at time t; $S_{\mathrm{MGs}}^{\mathrm{sell}}$, σ_t and κ_t are the electricity selling state, price and amount of microgrid i at time t; M is the number of game players; σ_{nt}, κ_{nt} are the auxiliary variables.

$H_{\mathrm{da}}(x, \sigma, \kappa) = 0$ and $G_{\mathrm{da}}(x, \sigma, \kappa) \leq 0$ are the day-ahead equality and inequality constraints, which consist of the bidding constraints, the CGs operation constraints, the energy storage system operation constraints, the day-ahead energy balance constraints, the DN interaction constraints and the interaction constraints with other microgrids.

1) Bidding constraints

The microgrid with power deficit successively trades with microgrids with surplus power according to the bidding prices from low to high until the demand-generation balance is achieved. Therefore, the bidding amount is related with the bidding price. Game microgrid i formulates the bidding strategy according to its own operation condition and the broadcast bidding strategies of other game players. At time t, microgrid i arranges the electricity bidding prices of other game microgrids in ascending order and the price set can be denoted as $\{\overline{\sigma}_{1t}, \overline{\sigma}_{2t}, \cdots, \overline{\sigma}_{nt}\}$. The electricity bidding amounts of other game microgrids are arranged corresponding to the above bidding price set $\{\overline{\sigma}_{1t}, \overline{\sigma}_{2t}, \cdots, \overline{\sigma}_{nt}\}$, and the amount set can be described as $\{\overline{\kappa}_{1t}, \overline{\kappa}_{2t}, \cdots, \overline{\kappa}_{nt}\}$. The bidding price and the bidding amount of microgrid i at time t has n possible states. Therefore, the bidding price set $\{\sigma_{i,1t}, \sigma_{i,2t}, \cdots, \sigma_{\mathrm{i,nt}}\}$, the bidding amount set $\{\kappa_{i,1t}, \kappa_{i,2t}, \cdots, \kappa_{\mathrm{i,nt}}\}$ and the state set $\{S_{1t}, S_{2t}, \cdots, S_{nt}\}$ of microgrid i at time t are presented for the bidding strategy formulation. $S_{1t} + S_{2t} + \cdots S_{nt} \leq 1$. If $S_{2t} = 1$, the bidding price $\sigma_{i,t}$ of microgrid i at time t is at the interval $[\overline{\sigma}_{1t}, \overline{\sigma}_{2t}]$, where $\overline{\sigma}_{1t}$ and $\overline{\sigma}_{2t}$ are the lowest and the second lowest bidding prices of the other game microgrids. The bidding amount $\kappa_{i,t}$ of microgrid i at time t is at the interval $[0, \kappa_t^{\mathrm{all}} - \overline{\kappa}_{1t}]$, where κ_t^{all} is the total amount of electricity purchased from MMS at time t, $\overline{\kappa}_{1t}$ is the electricity bidding amount of other game microgrids with the lowest bidding price.

$$\begin{cases} 0 \leq \sigma_{i,1t} \leq \overline{\sigma}_{1t} S_{1t} \\ \overline{\sigma}_{1t} \leq \sigma_{i,2t} \leq \overline{\sigma}_{2t} S_{2t} \\ \quad \cdots \\ \overline{\sigma}_{(n-1)t} \leq \sigma_{\mathrm{i,nt}} \leq \overline{\sigma}_{nt} S_{nt} \\ 0 \leq \kappa_{i,1t} \leq \kappa_t^{\mathrm{all}} S_{1t} \\ 0 \leq \kappa_{i,2t} \leq (\kappa_t^{\mathrm{all}} - \overline{\kappa}_{1t}) S_{2t} \\ \quad \cdots \\ 0 \leq \kappa_{\mathrm{i,nt}} \leq (\kappa_t^{\mathrm{all}} - \overline{\kappa}_{1t} - \cdots - \overline{\kappa}_{(n-1)t}) S_{2t} \\ S_{1t} + S_{2t} + \cdots S_{nt} \leq 1 \end{cases} \tag{6}$$

2) CGs operation constraints

$$\begin{cases} 0 \leq P_{(\mathrm{CG},i)}(t) \leq S_{(\mathrm{CG},i)}(t) \cdot P_{(\mathrm{CG},i)}^{\max} \\ -R_{(\mathrm{CG},i)}^{\mathrm{down}} \leq P_{(\mathrm{CG},i)}(t) - P_{(\mathrm{CG},i)}(t-1) \leq R_{(\mathrm{CG},i)}^{\mathrm{up}} \end{cases} \tag{7}$$

where $S_{(\mathrm{CG},i)}(t)$ and $P_{(\mathrm{CG},i)}(t)$ are the operation status and output of CG in the day-ahead stage; $R_{(\mathrm{CG},i)}^{\mathrm{up}}$ and $R_{(\mathrm{CG},i)}^{\mathrm{down}}$ are the maximum up and down ramping capacities.

3) Energy storage system operation constraints

$$\begin{aligned} & 0 \leq P_{(\mathrm{SS},i,\mathrm{DA})}^{\mathrm{ch}}(t) \leq S_{(\mathrm{SS},i,\mathrm{DA})}^{\mathrm{ch}}(t) \cdot P_{\mathrm{SS},i}^{(\mathrm{ch,max})} \\ & 0 \leq P_{(\mathrm{SS},i,\mathrm{DA})}^{\mathrm{dis}}(t) \leq S_{(\mathrm{SS},i,\mathrm{DA})}^{\mathrm{dis}}(t) \cdot P_{\mathrm{SS},i}^{(\mathrm{dis,max})} \\ & E_{(\mathrm{SS},i,\mathrm{DA})}(t) = (1 - \delta_{(\mathrm{SS},i)}) \cdot E_{(\mathrm{SS},i,\mathrm{DA})}(t-1) \\ & \quad + \left[\eta_{(\mathrm{SS},i)}^{\mathrm{ch}} \cdot P_{(\mathrm{SS},i,\mathrm{DA})}^{\mathrm{ch}}(t-1) - \frac{P_{(\mathrm{SS},i,\mathrm{DA})}^{\mathrm{dis}}(t-1)}{\eta_{(\mathrm{SS},i)}^{\mathrm{dis}}} \right] \cdot \Delta t \\ & E_{(\mathrm{SS},i)}^{\min} \leq E_{(\mathrm{SS},i,\mathrm{DA})}(t) \leq E_{(\mathrm{SS},i)}^{\max} \\ & E_{(\mathrm{SS},i,\mathrm{DA})}(T) = E_{(\mathrm{SS},i,\mathrm{DA})}(0) \end{aligned} \tag{8}$$

where $S_{(\mathrm{SS},i,\mathrm{DA})}^{\mathrm{ch}}(t)$ and $S_{(\mathrm{SS},i,\mathrm{DA})}^{\mathrm{dis}}(t)$ are the 0–1 variables which represent the charging and discharging states in the day-ahead stage; $P_{(\mathrm{SS},i,\mathrm{DA})}^{\mathrm{ch}}(t)$ and $P_{(\mathrm{SS},i,\mathrm{DA})}^{\mathrm{dis}}(t)$ are the charging and discharging power at time t; $E_{(\mathrm{SS},i,\mathrm{DA})}(t)$ is the stored energy at time t; $\delta_{(\mathrm{SS},i)}$, $\eta_{(\mathrm{SS},i)}^{\mathrm{ch}}$ and $\eta_{(\mathrm{SS},i)}^{\mathrm{dis}}$ are the attrition rate, and charging and discharging efficiency respectively.

4) DN interaction constraints

$$\begin{cases} 0 \leq P_{\mathrm{Grid},i}^{\mathrm{buy}}(t) \leq S_{\mathrm{Grid},i}^{\mathrm{buy}}(t) \cdot P_{\mathrm{Grid},i}^{(\mathrm{buy,max})} \\ 0 \leq P_{\mathrm{Grid},i}^{\mathrm{sell}}(t) \leq S_{\mathrm{Grid},i}^{\mathrm{sell}}(t) \cdot P_{\mathrm{Grid},i}^{(\mathrm{sell,max})} \end{cases} \tag{9}$$

where $S_{\mathrm{Grid},i}^{\mathrm{buy}}(t)$ and $S_{\mathrm{Grid},i}^{\mathrm{sell}}(t)$ are the purchasing and selling states of microgrid i with DN; $P_{\mathrm{Grid},i}^{(\mathrm{buy,max})}$ and $P_{\mathrm{Grid},i}^{(\mathrm{sell,max})}$ are the maximum purchasing and selling power.

5) Interaction constraints with other microgrids

$$\begin{cases} 0 \leq P_{\mathrm{MGs},i}^{\mathrm{buy}}(t) \leq S_{\mathrm{MGs},i}^{\mathrm{buy}}(t) \cdot P_{\mathrm{MGs},i}^{(\mathrm{buy,max})} \\ 0 \leq P_{\mathrm{MGs},i}^{\mathrm{sell}}(t) \leq S_{\mathrm{MGs},i}^{\mathrm{sell}}(t) \cdot P_{\mathrm{MGs},i}^{(\mathrm{sell,max})} \end{cases} \tag{10}$$

where $S_{\mathrm{MGs},i}^{\mathrm{buy}}(t)$ and $S_{\mathrm{MGs},i}^{\mathrm{sell}}(t)$ are the purchasing and selling states of microgrid i with other microgrids; $P_{\mathrm{MGs},i}^{\mathrm{buy}}(t)$ and $P_{\mathrm{MGs},i}^{\mathrm{sell}}(t)$ are the purchasing and selling power.

6) Day-ahead energy balance constraints

$$\begin{aligned} & P_{\mathrm{MT}}(t) + P_{\mathrm{FC}}(t) + P_{(\mathrm{SS},i,\mathrm{DA})}^{\mathrm{dis}}(t) + P_{\mathrm{wind}}^{\mathrm{pre}}(t) + P_{\mathrm{Grid},i}^{\mathrm{buy}}(t) \\ & + P_{\mathrm{MGs},i}^{\mathrm{buy}}(t) = P_{\mathrm{Load}}(t) + P_{(\mathrm{SS},i,\mathrm{DA})}^{\mathrm{ch}}(t) + P_{\mathrm{Grid},i}^{\mathrm{sell}}(t) + \kappa_t \end{aligned} \tag{11}$$

B. Real-time Stage of the Two-stage ARG-BD Model

The real-time stage of the individual microgrid two-stage ARG-BD model can be represented by (12):

$$\begin{cases} \min\limits_{x,\sigma,\kappa} \{ \max\limits_{u} \min\limits_{y} C_{\mathrm{rt}}(u, y) \} \\ \text{s.t.} \quad H_{\mathrm{rt}}(x, \sigma, \kappa, u, y, \Gamma) = 0 \\ \qquad G_{\mathrm{rt}}(x, \sigma, \kappa, u, y, \Gamma) \leq 0 \end{cases} \tag{12}$$

The real-time stage model is formulated in the "max-min" form, in which the "max" layer searches for the worst-case scenario of WPG based on the optimal bidding strategy (σ, κ) and the day-ahead economic dispatch strategy x achieved in the day-ahead stage, the "min" layer seeks the corresponding adjustment strategy y.

The real-time adjustment cost $C_{\mathrm{rt}}(u, y)$ consists of the regulation costs and of CGs, the real-time grid interaction cost and the wind curtailment cost, of which the details are shown as follows:

$$\begin{aligned} C_{\mathrm{rt}}(u, y) &= C_{\mathrm{CG}}^{\mathrm{up}} + C_{\mathrm{CG}}^{\mathrm{down}} + C_{\mathrm{Balance}} + C_{\mathrm{Wind}}^{\mathrm{loss}} \\ C_{\mathrm{CG}}^{\mathrm{up}} &= \sum_i \sum_t [\lambda_{(\mathrm{CG},i)}^{\mathrm{up}} \cdot P_{(\mathrm{CG},i)}^{\mathrm{up}}(t)] \cdot \Delta t \\ C_{\mathrm{CG}}^{\mathrm{down}} &= \sum_i \sum_t [\lambda_{(\mathrm{CG},i)}^{\mathrm{down}} \cdot P_{(\mathrm{CG},i)}^{\mathrm{down}}(t)] \cdot \Delta t \\ C_{\mathrm{Balance}} &= \sum_t [\lambda_{\mathrm{Balance}}^{\mathrm{buy}}(t) P_{\mathrm{Balance}}^{\mathrm{buy}}(t) \\ & \quad - \lambda_{\mathrm{Balance}}^{\mathrm{sell}}(t) P_{\mathrm{Balance}}^{\mathrm{sell}}(t)] \cdot \Delta t \end{aligned}$$

$$C_{\mathrm{Wind}}^{\mathrm{loss}} = \sum_t \lambda_{\mathrm{Wind}}^{\mathrm{loss}} \cdot [P_{\mathrm{Wind}}(t) - P_{\mathrm{Wind}}^{\mathrm{get}}(t)] \cdot \Delta t \quad (13)$$

where $\lambda_{(\mathrm{CG},i)}^{\mathrm{up}}$ and $\lambda_{(\mathrm{CG},i)}^{\mathrm{down}}$ are the up and down regulation prices of CG; $P_{(\mathrm{CG},i)}^{\mathrm{up}}(t)$ and $P_{(\mathrm{CG},i)}^{\mathrm{down}}(t)$ are the up and down regulation power; $\lambda_{\mathrm{Balance}}^{\mathrm{buy}}(t)$ and $\lambda_{\mathrm{Balance}}^{\mathrm{sell}}(t)$ are the purchasing and selling prices from DN in the real-time market; $P_{\mathrm{Balance}}^{\mathrm{buy}}(t)$ and $P_{\mathrm{Balance}}^{\mathrm{sell}}(t)$ are the purchased and sold power of microgrid i; $\lambda_{\mathrm{Wind}}^{\mathrm{loss}}$ is the wind penalty prices; $P_{\mathrm{Wind}}(t)$ is the actual output of WPG; $P_{\mathrm{Wind}}^{\mathrm{get}}(t)$ is the actual injected WPG.

$H_{\mathrm{rt}}(x, \sigma, \kappa, u, y, \Gamma) = 0$ and $G_{\mathrm{rt}}(x, \sigma, \kappa, u, y, \Gamma) \leq 0$ are the real-time equality and inequality constraints, which consist of the WPG constraints, the CGs real-time regulation constraints, the real-time DN interaction constraints and the real-time energy balance constraints.

1) WPG constraints

$$0 \leq P_{\mathrm{Wind}}^{\mathrm{get}}(t) \leq P_{\mathrm{Wind}}(t) \quad (14)$$

2) CGs real-time regulation constraints

$$\begin{aligned} & 0 \leq P_{(\mathrm{CG},i)}^{\mathrm{up}}(t) \leq P_{(\mathrm{CG},i)}^{(\mathrm{up.max})} \\ & 0 \leq P_{(\mathrm{CG},i)}^{\mathrm{down}}(t) \leq P_{(\mathrm{CG},i)}^{(\mathrm{down.max})} \\ & -R_{(\mathrm{CG},i)}^{\mathrm{down}} \leq P_{(\mathrm{CG},i)}(t) + P_{(\mathrm{CG},i)}^{\mathrm{up}}(t) - P_{(\mathrm{CG},i)}^{\mathrm{down}}(t) \\ & \quad - [P_{(\mathrm{CG},i)}(t-1) + P_{(\mathrm{CG},i)}^{\mathrm{up}}(t-1) - P_{(\mathrm{CG},i)}^{\mathrm{down}}(t-1)] \\ & \leq R_{(\mathrm{CG},i)}^{\mathrm{up}} \end{aligned} \quad (15)$$

3) Real-time DN interaction constraints

$$\begin{cases} 0 \leq P_{\mathrm{Balance}}^{\mathrm{buy}}(t) \leq P_{\mathrm{Balance}}^{(\mathrm{buy,max})} \\ 0 \leq P_{\mathrm{Balance}}^{\mathrm{sell}}(t) \leq P_{\mathrm{Balance}}^{(\mathrm{sell,max})} \\ 0 \leq P_{\mathrm{Grid}}^{\mathrm{buy}}(t) + P_{\mathrm{Balance}}^{\mathrm{buy}}(t) \leq P_{\mathrm{Grid}}^{(\mathrm{buy,max})} \\ 0 \leq P_{\mathrm{Grid}}^{\mathrm{sell}}(t) + P_{\mathrm{Balance}}^{\mathrm{sell}}(t) \leq P_{\mathrm{Grid}}^{(\mathrm{sell,max})} \end{cases} \quad (16)$$

4) Real-time energy balance constraints

$$\begin{aligned} & P_{\mathrm{MGs},i}^{\mathrm{buy}}(t) + P_{\mathrm{MT}}(t) + P_{\mathrm{MT}}^{\mathrm{up}}(t) - P_{\mathrm{MT}}^{\mathrm{down}}(t) + P_{\mathrm{FC}}(t) \\ & \quad + P_{\mathrm{FC}}^{\mathrm{up}}(t) - P_{\mathrm{FC}}^{\mathrm{down}}(t) + P_{(\mathrm{SS},i,\mathrm{RT})}^{\mathrm{dis}}(t) + P_{\mathrm{wind}}^{\mathrm{get}}(t) \\ & \quad + P_{\mathrm{Grid},i}^{\mathrm{buy}}(t) + P_{\mathrm{Balance}}^{\mathrm{buy}}(t) \\ & = P_{\mathrm{Load}}(t) + P_{(\mathrm{SS},i,\mathrm{RT})}^{\mathrm{ch}}(t) + P_{\mathrm{Grid},i}^{\mathrm{sell}}(t) + P_{\mathrm{Balance}}^{\mathrm{sell}}(t) + \kappa_t \end{aligned} \quad (17)$$

IV. Model Solution

A. Detailed Solution of the Individual Microgrid Two-stage ARG-BD Model

The model is able to be rewritten in the following matrix form:

$$\begin{cases} \min\limits_{\boldsymbol{x},\boldsymbol{\sigma},\boldsymbol{\kappa}} \{\boldsymbol{c}^{\mathrm{T}}(\boldsymbol{x},\boldsymbol{\sigma},\boldsymbol{\kappa}) + \max\limits_{\boldsymbol{u}} \min\limits_{\boldsymbol{y}} (\boldsymbol{d}^{\mathrm{T}}\boldsymbol{y} + \boldsymbol{e}^{\mathrm{T}}\boldsymbol{u})\} \\ \text{s.t.} \quad \boldsymbol{A}\boldsymbol{x} = \boldsymbol{g}, \boldsymbol{B}\boldsymbol{x} \leq \boldsymbol{h} \\ \quad\quad \boldsymbol{C}\boldsymbol{x} + \boldsymbol{D}\boldsymbol{y} = \boldsymbol{i}, \boldsymbol{E}\boldsymbol{x} + \boldsymbol{F}\boldsymbol{y} \leq \boldsymbol{j} \\ \quad\quad \boldsymbol{G}\boldsymbol{y} \leq \boldsymbol{u} \end{cases} \quad (18)$$

where $\boldsymbol{c}$, $\boldsymbol{d}$, $\boldsymbol{e}$ are the coefficient matrices in the objectives; $\boldsymbol{A}$, $\boldsymbol{C}$, $\boldsymbol{D}$ are the coefficient matrices of the equality constraints; $\boldsymbol{g}$, $\boldsymbol{i}$ are the constant column vectors of the equality constraints; $\boldsymbol{B}$, $\boldsymbol{E}$, $\boldsymbol{F}$, $\boldsymbol{G}$ are the coefficient matrices of thr inequality constraints; $\boldsymbol{h}$, $\boldsymbol{j}$ are the constant column vectors of the inequality constraints.

The decomposed master problem searches for the optimal bidding strategy (σ, κ) and the day-ahead economic dispatch strategy x, which is able to be explained by (19):

$$\begin{cases} \min\limits_{\boldsymbol{x},\boldsymbol{\sigma},\boldsymbol{\kappa}} \{\boldsymbol{c}^{\mathrm{T}}(\boldsymbol{x},\boldsymbol{\sigma},\boldsymbol{\kappa}) + \theta\} \\ \text{s.t.} \quad \theta \geq \boldsymbol{d}^{\mathrm{T}}\boldsymbol{y} + \boldsymbol{e}^{\mathrm{T}}\boldsymbol{u} \\ \quad\quad \boldsymbol{A}\boldsymbol{x} = \boldsymbol{g}, \boldsymbol{B}\boldsymbol{x} \leq \boldsymbol{h} \\ \quad\quad \boldsymbol{C}\boldsymbol{x} + \boldsymbol{D}\boldsymbol{y} = \boldsymbol{i} \\ \quad\quad \boldsymbol{E}\boldsymbol{x} + \boldsymbol{F}\boldsymbol{y} \leq \boldsymbol{j} \\ \quad\quad \boldsymbol{G}\boldsymbol{y} \leq \boldsymbol{u} \end{cases} \quad (19)$$

The master problem cannot be solved directly due to the bilinear item $\sigma_t \kappa_t$ in the objective function. Therefore, the binary expansion method is utilized to linearize the bilinear term:

$$\begin{cases} \sigma_t \kappa_t = \sigma_{tb}^{\min} \kappa_t + \Delta\sigma \sum\limits_{b=0}^{B_\sigma} 2^b v_{tb} \\ \sigma_{tb}^{\min} \kappa_t + \Delta\sigma \sum\limits_{b=0}^{B_\sigma} 2^b x_{tb} \leq \sigma_{tb}^{\max} \\ v_{tb} = x_{tb} \kappa_t \\ \Delta\sigma = (\sigma_{tb}^{\max} - \sigma_{tb}^{\min})/M_1 \\ M_1 = 2^{B_\sigma} \\ 0 \leq \kappa_t - v_{tb} \leq M_\sigma (1 - x_{tb}) \end{cases} \quad (20)$$

where $\sigma_{tb}^{\min}$ and $\sigma_{tb}^{\max}$ are the minimum and maximum electricity bidding prices; v_{tb} is the auxiliary variable; x_{tb} is the introduced binary variable; B_σ is the number of binary variables; M_σ is a sufficiently large constant.

The decomposed "max-min" sub-problem seeks the WPG worst-case scenario u and the corresponding real-time adjustment strategy y, which can be represented by (21):

$$\begin{cases} \min\limits_{\boldsymbol{x},\boldsymbol{\sigma},\boldsymbol{\kappa}} \{\max\limits_{\boldsymbol{u}} \min\limits_{\boldsymbol{y}} (\boldsymbol{d}^{\mathrm{T}}\boldsymbol{y} + \boldsymbol{e}^{\mathrm{T}}\boldsymbol{u})\} \\ \text{s.t.} \quad \boldsymbol{C}\boldsymbol{x} + \boldsymbol{D}\boldsymbol{y} = \boldsymbol{i} \\ \quad\quad \boldsymbol{E}\boldsymbol{x} + \boldsymbol{F}\boldsymbol{y} \leq \boldsymbol{j} \\ \quad\quad \boldsymbol{G}\boldsymbol{y} \leq \boldsymbol{u} \end{cases} \quad (21)$$

Duality theory and the Big M method are applied to dual and linearize the decomposed "max-min" sub-problem. The transformed model can be depicted by (22). The detailed transformation process can be referred to in [44].

$$\begin{aligned} & \max_{\boldsymbol{u},\boldsymbol{\alpha},\boldsymbol{\beta},\boldsymbol{\gamma}} \boldsymbol{u}^{\mathrm{up}}\boldsymbol{\xi}^{+} + \boldsymbol{u}^{\mathrm{down}}\boldsymbol{\xi}^{-} + \boldsymbol{u}^{\mathrm{pre}}(1 - \boldsymbol{\xi}^{+} - \boldsymbol{\xi}^{-}) \\ & \quad\quad + \boldsymbol{i}^{\mathrm{T}}\boldsymbol{\alpha} - \boldsymbol{x}^{\mathrm{T}}\boldsymbol{C}^{\mathrm{T}}\boldsymbol{\alpha} + \boldsymbol{j}^{\mathrm{T}}\boldsymbol{\beta} - \boldsymbol{x}^{\mathrm{T}}\boldsymbol{E}^{\mathrm{T}}\boldsymbol{\beta} \\ & \text{s.t.} \quad \boldsymbol{D}^{\mathrm{T}}\boldsymbol{\alpha} + \boldsymbol{F}^{\mathrm{T}}\boldsymbol{\beta} + \boldsymbol{G}^{\mathrm{T}}\boldsymbol{\gamma} = \boldsymbol{d}, \boldsymbol{\xi} = \boldsymbol{e} + \boldsymbol{\gamma}, \boldsymbol{\beta} \leq 0, \boldsymbol{\gamma} \leq 0 \\ & \quad\quad - M(1 - \mu_i^{+}) + \xi_i \leq \xi_i^{+} \leq -M(1 - \mu_i^{+}) + \xi_i \\ & \quad\quad - M(1 - \mu_i^{-}) + \xi_i \leq \xi_i^{-} \leq -M(1 - \mu_i^{-}) + \xi_i \\ & \quad\quad - M\mu_i^{+} \leq \xi_i^{+} \leq M\mu_i^{+} \\ & \quad\quad - M\mu_i^{-} \leq \xi_i^{-} \leq M\mu_i^{-} \end{aligned}$$

$$\mu_i^+ + \mu_i^- \leq 1, \sum_i (\mu_i^+ + \mu_i^-) \leq \Gamma \tag{22}$$

The major steps of the iteration process between the master problem and the sub-problem are listed in Table II.

TABLE II
THE MAJOR STEPS OF THE ITERATION PROCESS

The major steps of the iteration process	
Step 1	Initialize the upper and lower bounds $U_0 = +\infty$, $L_0 = -\infty$. Set the initial scenario $\boldsymbol{u}_1$, the value of the convergence gap λ, and the iteration number $k = 1$.
Step 2	Solve the master problem considering the known worst-case scenario set $\boldsymbol{u}_l$. Get the optimal solution $(\boldsymbol{x}_k, \boldsymbol{\sigma}_k, \boldsymbol{\kappa}_k)$ and set the master problem objective as the new lower bound L_k.
Step 3	Solve the sub-problem based on $(\boldsymbol{x}_k, \boldsymbol{\sigma}_k, \boldsymbol{\kappa}_k)$ achieved in Step 2. Get the optimal solution $(\boldsymbol{u}_k^{\mathrm{o}}, \boldsymbol{y}_k^{\mathrm{o}})$ and update the worst-case scenario set $\boldsymbol{u}_{k+1} = \boldsymbol{u}_k^{\mathrm{o}}$. Set the sum of sub-problem objective and main problem $\boldsymbol{c}^{\mathrm{T}}(\boldsymbol{x}, \boldsymbol{\sigma}, \boldsymbol{\kappa})$ as the new upper bound U_k.
Step 4	If $U_k - L_k \leq \lambda$, get the optimal solution $(\boldsymbol{x}_k, \boldsymbol{\sigma}_k, \boldsymbol{\kappa}_k)$. Otherwise, update $k = k+1$ and go back to Stepthe2.

B. Alternating Robust-game Procedure

The presented MMS robust-game model includes the intra-microgrid operation and inter-microgrid game. During every round of the game, each microgrid employs the individual two-stage ARG-BD model to achieve the optimal DA-BD strategy. When obtaining the Nash equilibrium solution, the alternating robust-game procedure stops. The detailed steps of the alternating robust-game procedure are shown in Fig. 4. The blue part of the flow chart describes the whole game process of the presented MMS robust-game model, which is run on-chain to achieve the complete information game environment. The grey part of the flow chart illustrates the specific DA-BD strategy formulation process, which is accomplished by the individual microgrid system and run off-chain.

V. CASE STUDY

The presented blockchain-enabled robust-game electricity transaction model is tested on a decentralized electricity trading platform, which is built based on the ethereum client Ganache, Remix online compiler and Metamask wallet. A private chain is first created in Ganache, and the smart contracts describing MMS transaction rules are compiled and deployed in the private chain by using the Remix online complier. A Metamask wallet is adopted to record the transaction process. All individual microgrids in MMS jointly negotiate and decide

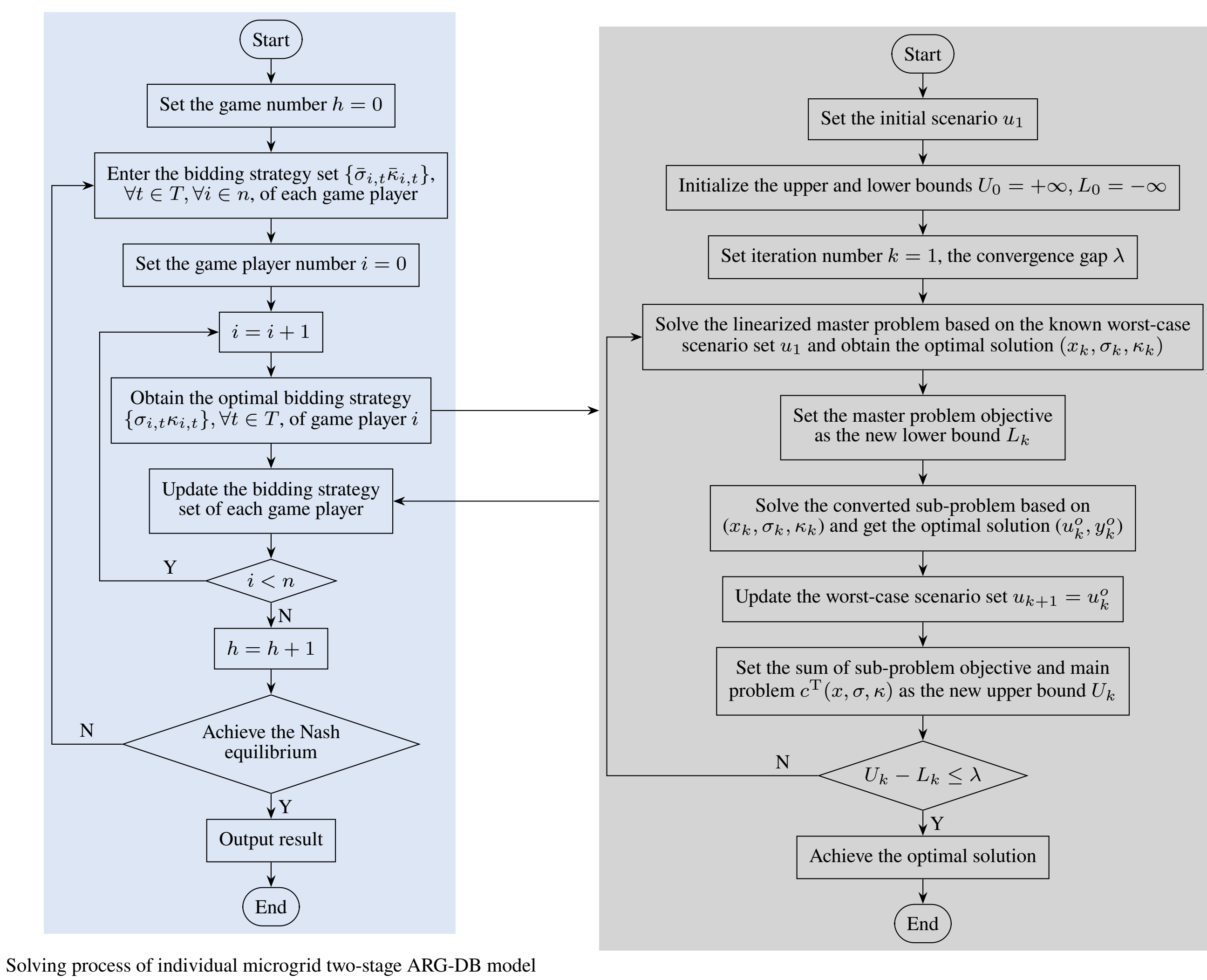

Fig. 4. Alternating robust-game procedure.

the conversion rate between the electricity trading platform token and the dollar. 1 ether is equivalent to $1 as the primary setting. The MMS includes one microgrid with a power deficit and three microgrids with surplus power. The electricity purchase demand, load demand and predicted WPG of the microgrid with power deficit in each time period are shown in Fig. 5. The predicted WPG and load demand of microgrids with surplus power are respectively shown in Figs. 6, and 7. The parameters of CGs and the energy storage system in each microgrid are respectively shown in Tables III and IV.

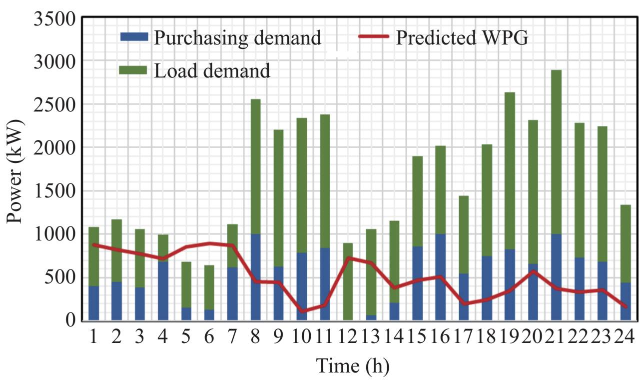

Fig. 5. Purchase demand, load demand and predicted WPG of the purchasing MG.

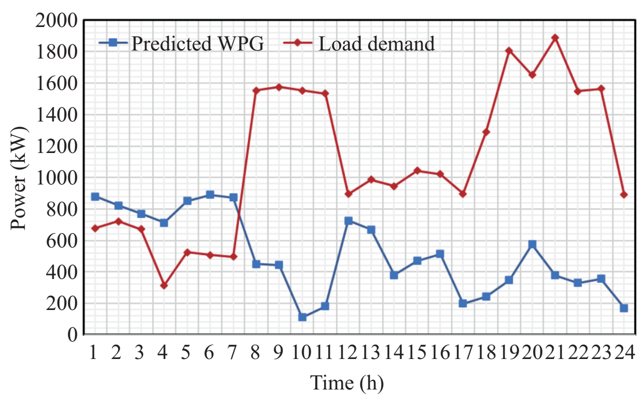

Fig. 6. Load demand and predicted WPG of the selling MG 1.

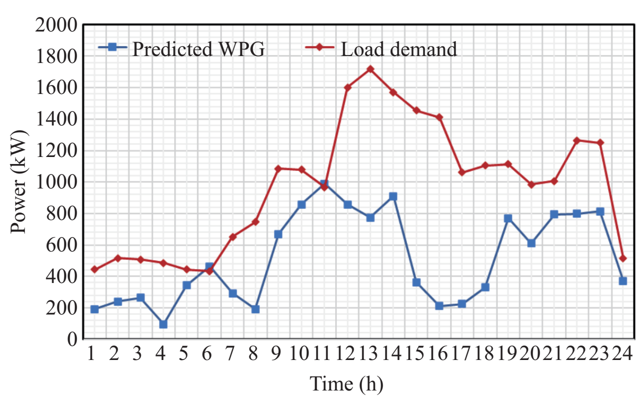

Fig. 7. Load demand and predicted WPG of the selling MG 2.

TABLE III
THE PARAMETERS OF CGS

Description	Rated capacity (kW h)	Ramp rate (kW $\min^{-1}$)	Generation cost ($/kW)	Regulation cost ($/kW)
Selling MG 1-MT	600	6	0.67	1.005
Selling MG 1-FC	600	2	0.60	0.900
Selling MG 2-MT	800	6	0.67	1.005
Selling MG 2-FC	400	2	0.60	0.900
Selling MG 3-MT	400	6	0.67	1.005
Selling MG 3-FC	800	2	0.60	0.900
Purchasing MG-MT	600	6	0.67	1.005
Purchasing MG-FC	600	2	0.60	0.900

TABLE IV
THE PARAMETERS OF ENERGY STORAGE SYSTEM

Description	Selling MG 1	Selling MG 2	Selling MG 3	Purchasing MG
Rated Capacity (kWh)	800	600	400	800
Maximum Charging and Discharging Power (kW)	250	200	150	250
Self-Loss Coefficient	0.999	0.999	0.999	0.999
Charging Coefficient	0.900	0.900	0.900	0.900
Discharge Coefficient	0.900	0.900	0.900	0.900

TABLE V
THE PARAMETERS OF WIND POWER GENERATORS

Description	Selling MG 1	Selling MG 2	Selling MG 3	Purchasing MG
Rated capacity (kW h)	1000	1200	1200	1000
Penalty price ($/kW h)	0.536	0.536	0.536	0.536

A. Trading Result Analysis

In the blockchain-enabled complete information game environment, the three microgrids with surplus power set the adjustable robust parameters of the WPG uncertain interval to 10, and the prediction errors to 10 %. Based on the electricity purchase demand released by the microgrid with power deficit, the three game players achieve the Nash equilibrium solution of the MMS robust-game model after nine rounds of games.

1) Economy and WPG consumption analysis

The comparison of the overall economy and WPG consumption is illustrated in Table VI. The obtained bidding prices of the three game players are shown in Fig. 8.

TABLE VI
COMPARISON OF ECONOMY AND WIND POWER CONSUMPTION

Description	With MMS electricity transaction		Without MMS electricity transaction	
	Day-ahead operation cost ($)	Wind curtailment (kWh)	Day-ahead operation cost ($)	Wind curtailment (kWh)
MMS	35512.4	60.2	40126.7	133.2
Selling MG 1	9714.6	0	10045.5	0
Selling MG 2	4766.6	43.3	6154.4	81.4
Selling MG 3	4314.1	16.9	5808.4	51.8
Purchasing MG 4	16717.1	0	18118.7	0

Figure 8 demonstrates that the maximum and minimum electricity bidding prices are both lower than the selling price of DN and higher than the purchase price of DN in each

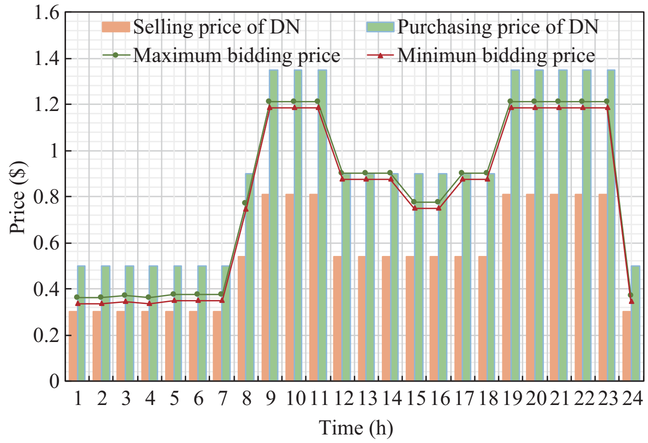

Fig. 8. Obtained bidding prices of game players.

time period. Combined with Table VI, it can be seen that when the bidding price is within the range of the selling and purchase prices of DN, the microgrids with surplus power can increase the electricity selling profit, the microgrid with power deficit is able to reduce the electricity purchase cost, and the overall economy improvement can be achieved. Table VI also indicates that the MMS electricity transaction is able to reduce the wind curtailment and promote WPG consumption.

2) Optimization result analysis

The optimization results of the microgrids with surplus power are shown in Table VII, and the electricity bidding amounts of each game players are illustrated in Fig. 9.

Table VII indicates that the power supply of selling microgrid 1 is insufficient at some time period, so it is necessary to purchase electricity from DN to ensure the supply-demand balance. After selling power to MMS, selling microgrid 1

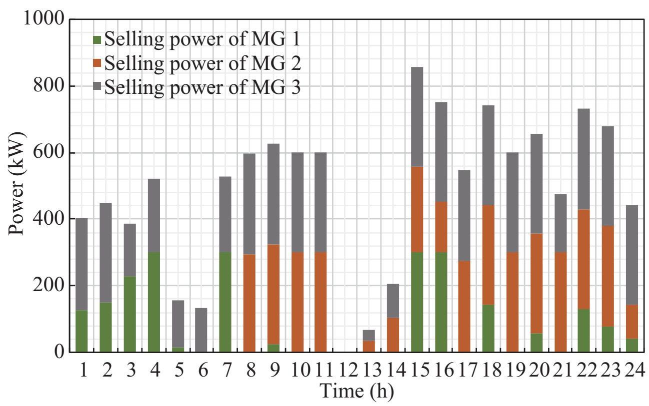

Fig. 9. Electricity bidding amount of each game player.

TABLE VII
OPTIMIZATION RESULT OF MICROGRIDS WITH SURPLUS POWER

Description		Selling MG 1	Selling MG 2	Selling MG 3
Day-ahead operation cost ($)	MT	5077.8	7472.4	2991.4
	FC	5834.7	3560.3	7392.5
	DN	117.4	−2140.0	−1335.9
	Bidding profit	1315.3	4126.1	4733.9
Real-time adjustment cost ($)		612.1	710.1	715.2
Total operation cost ($)		10326.7	5476.7	5029.3

and microgrid 2 still have surplus power that can be sold to DN for additional profit. In the complete information game environment, the bidding profits of selling microgrid 1 and microgrid 2 account for the vast majority of the total bidding income of MMS. Combining with Fig. 9, it can be seen that the electricity bidding amount of selling microgrid 1 is the least, and it is concentrated in the time period 1:00–7:00 and 15:00–16:00 with the relatively low bidding prices, that is, less electricity is sold at lower prices. Selling microgrid 2 and microgrid 3 achieve a dominant position in the game competition, selling more electricity at 8:00–11:00 and 17:00–23:00 when the bidding prices are relatively high. As can be seen from Table VII and Fig. 9, the microgrids with more surplus power occupy more dominant positions in the game. This is due to the fact that the surplus power can be transferred and stored through the flexible operation and regulation behaviors of the microgrid, and it can be sold at the time period when the purchase demand is large or the price is high to achieve satisfactory bidding profit.

3) DA-BD strategy analysis

Figures 10, 11 and 12 show the DA-BD strategies of each selling microgrid. The DA-BD strategy includes the day-ahead output of CGs, the transaction strategy with DN, the electricity bidding price and amount. The results of the MMS robust-game model can be analyzed from the perspective of the specific operation behaviors of MMS. Each selling microgrid

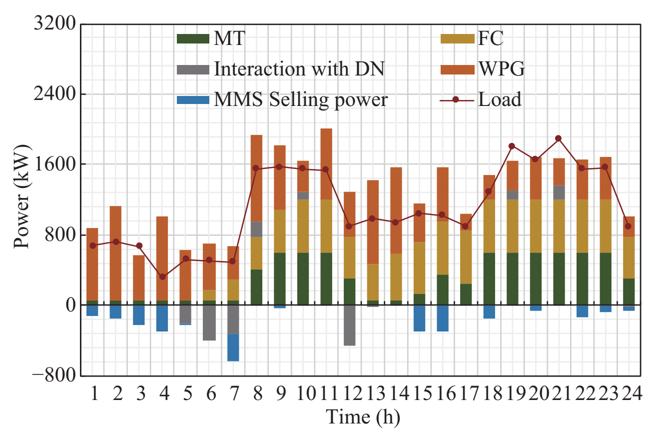

Fig. 10. Unit outputs of selling MG 1.

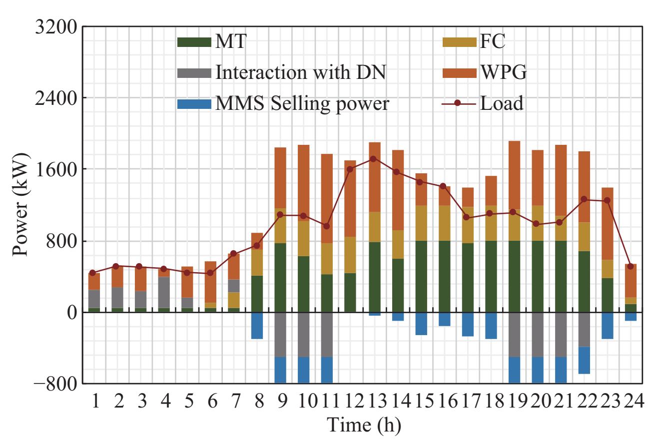

Fig. 11. Unit outputs of selling MG 2.

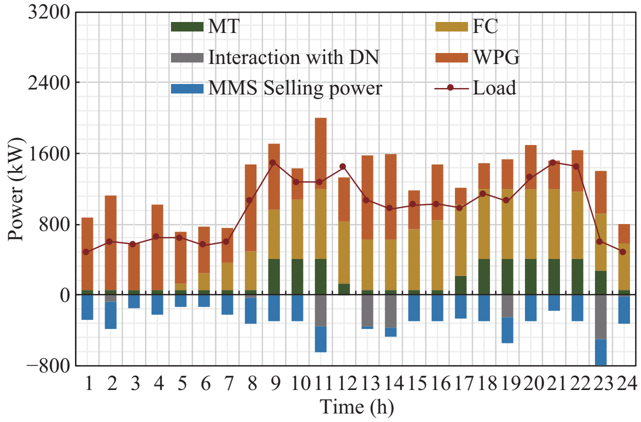

Fig. 12. Unit outputs of selling MG 3.

has the same installed capacity of CGs. CGs include the MT with higher generation cost and the FC with lower generation cost.

In selling microgrid 3, the installed capacity of FC is the largest, and the WPG output is relatively sufficient. Selling microgrid 3 is capable to be a storage for the surplus electricity when high WPG output or valley load demand comes, so it achieves a dominant position in the game competition. Load demand in selling microgrid 1 is larger than that of Selling microgrid 2 and microgrid 3. Although the capacity of the energy storage system in selling microgrid 1 is the largest, there is no surplus power to store and use at the appropriate time, so selling microgrid 1 is at a disadvantage in the game. Although the installed capacity of FC with lower generation cost is the smallest, selling microgrid 2 has the largest WPG output and its load demand is relatively small, so the satisfactory result has been achieved in the game process.

B. Transaction Procedure Based on Blockchain Technology

According to the electricity purchase demand released by the purchasing microgrid, the selling microgrids compete with each other to obtain the Nash equilibrium, which includes the optimal bidding strategy and the day-ahead economic dispatch strategy of each selling microgrid. The obtained Nash equilibrium triggers the preset response condition of energy trading smart contracts, and MMS conducts electricity transactions according to the pre-described energy trading rules. Taking the time period 16:00 as an example, the transaction process of MMS based on blockchain technology is shown in Tables VIII and IX.

Tables VIII and IX indicate that the electricity purchase demand of the purchasing microgrid at 16:00 cannot be fully satisfied through the transaction with the selling microgrids. To achieve the supply-demand balance, the purchasing microgrid still needs to buy electricity from DN after the MMS transaction. Based on the electricity trading rules, the purchasing microgrid conducts transactions with the selling microgrids according to the bidding prices from low to high, until the electricity purchase demand is satisfied. The purchasing microgrid first trades with the selling microgrid 1 at the price of 0.7494 (ether/kWh), and then trades with the selling microgrid

TABLE VIII
TRANSACTION INFORMATION OF MULTI-MICROGRID SYSTEM

Parties to transaction	Trading priceether (kWh)	Trading amount (kWh)
Purchasing MG-Selling MG1	0.7494	300.0
Purchasing MG-Selling MG2	0.7745	150.5
Purchasing MG-Selling MG3	0.7745	300.0
Purchasing MG-DN	0.9000	248.9

TABLE IX
TRANSACTION RESULT OF MULTI-MICROGRID SYSTEM

Trader	Trading address	Account balance before transaction (ether)	Account balance after transaction (ether)
Purchasing MG	0x9297...	10000.0	9202.2
Selling MG1	0xdB1f...	10000.0	10224.8
Selling MG1	0x5aE4...	10000.0	10116.6
Selling MG1	0x4a7e...	10000.0	10232.4
DN	0xe7Cc···	10000.0	10224.0

2 and microgrid 3 at the price of 0.7745 (ether/kWh). After the MMS transaction, the purchasing microgrid still has part of the unsatisfied electricity purchase demand, while the selling microgrids are constrained by their own operation conditions, and there is no extra electricity for sale. Therefore, the purchasing microgrid finally purchases electricity from DN at the price of 0.9000 (ether/kWh). The above results show that the smart contracts deployed on the blockchain platform can achieve the decentralized MMS transaction according to the pre-described energy trading rules.

C. Efficiency Comparison of Different Operation Modes

This paper simulates the MMS robust-game model under the centralized trading mechanism and the presented blockchain-enabled distributed trading mechanism in the MATLAB environment in order to compare their operation efficiency. Table X indicates that the MMS trading strategy formulation efficiency under the centralized trading mechanism is similar to that of the presented distributed trading mechanism. The reason is that the trading strategy formulation stage includes the individual microgrid trading strategy formulation process and the game information integration process. The calculation work is primarily concentrated in the individual microgrid trading strategy formulation process, which takes a lot of time to process the two-stage ARG-BD model. Under the presented blockchain-enabled distributed trading mechanism, game microgrids achieve a complete information game without intervention of a third trusted party. While under the centralized trading mechanism, each game microgrid uploads the obtained bidding strategy to the transaction center. The transaction center integrates and publishes the organized bidding information, providing references for the next round of games. The transaction center can quickly integrate and publish the bidding information since the structure of the interacted bidding strategy in the presented MMS robust-game model is simple. The trading time is from the moment of obtaining the Nash equilibrium of MMS robust-game model to the moment when the transaction block is generated. The trading

TABLE X
COMPARISON OF OPERATION TIME

Description	Trading strategy formulation stage				Transaction stage	
	Trading strategy formulation time	Single-round game time	Game information integration time	Total trading strategy formulation time	Single period trading time	Total trading time
Centralized transaction mode	23.80 s	89.82 s	0.756 ms	809.38 s	5.22 s	127.89 s
Decentralized transaction mode	23.80 s	89.82 s	–	809.38 s	1.47 ms	36.75 ms

TABLE XI
INFLUENCES OF WPG UNCERTAINTY ON OPERATION RESULT

Description	Considering WPG uncertainty				Ignoring WPG uncertainty			
	Bidding profit ($)	Day-ahead operation cost ($)	Expected real-time adjustment cost ($)	Expected total operation cost ($)	Bidding profit ($)	Day-ahead operation cost ($)	Expected real-time adjustment cost ($)	Expected total operation cost ($)
Selling MG 1	1315.3	9714.6	264.2	9978.8	1383.1	9686.8	432.8	10129.6
Selling MG 2	4126.10	4766.6	307.5	5074.1	4111.8	4664.6	480.2	5144.8
Selling MG 3	4733.9	4314.1	323.9	4638.0	4705.9	4286.0	508.4	4794.4

efficiency under the presented distributed trading mechanism is far superior to that of the centralized trading mechanism. This is due to the fact that the MMS electricity transaction smart contract embedded in the blockchain platform is automatically executed, and the decentralized and trusted transaction is achieved in an efficient way. In the trading strategy formulation stage, the blockchain-enable transaction platform provides a complete information game environment for all game microgrids without intervention of a third authority. In the transaction stage, the smart contract facilitates the decentralized, transparent and efficient MMS electricity transaction.

D. Influences of the WPG Uncertainty on the Transaction Model Results

Table XI indicates that the bidding profit of selling microgrid 1 increases when the WPG uncertainty is not taken into account. This is because the reserve capacity of CGs in selling microgrid 1 needs to be retained to deal with the WPG uncertainty. Therefore, the surplus power of selling microgrid 1 participating in the trading game decreases when considering WPG uncertainty. The ignorance of WPG uncertainty increases the surplus power and improves the bidding profit of selling microgrid 1. As the total electricity purchase demand is the same, the bidding profits of selling microgrid 2 and 3 decrease correspondingly when the WPG uncertainty is not taken into account. While the overall positions of the three selling microgrids in the game process remain unchanged. It also can be seen from Table XI that the ignorance of WPG uncertainty results in the lower day-ahead operation cost, higher real-time adjustment cost and total operation cost. The reason is that the deviation between the actual and predicted WPG in the real-time stage requires selling microgrids to adjust the obtained day-ahead bidding-dispatching strategies to achieve the real-time demand-generation balance. The DA-BD strategies, ignoring WPG uncertainty, costs more in the real-time stage.

E. Robustness Discussion of Individual Microgrid Two-stage ARG-BD Model

This section investigates the robustness and economy of the individual microgrid two-stage ARG-BD model in the presented MMS robust-game model. 1,000 random scenarios are generated to evaluate the performances of the DA-BD strategies obtained by using the presented two-stage ARG-BD model, deterministic-game bidding-dispatching (DG-BD) model and traditional robust-game bidding-dispatching (RG-BD) model. The adjustable robust parameter, representing the number of times that the worst-case scenario occurs, is set to 10. The prediction errors are set to 10 %. The total operation costs of the DA-BD strategies under 1,000 random scenarios are illustrated in Fig. 13. The comparison of specific operation costs are shown in Table XII.

Figure 13. indicates that the total operation costs of the ARG-BD strategy are less than the DG-BD strategy and RG-BD strategy in most scenarios. Combined with Table XII, it can be seen that the DG-BD strategy achieves the lowest day-ahead operation cost, and the RG-BD strategy obtains

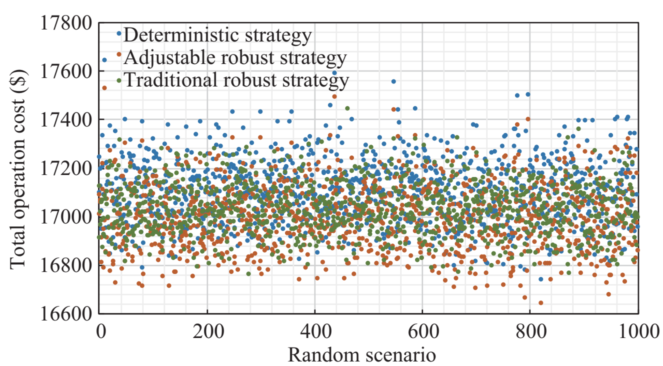

Fig. 13. Scatter of total operation costs.

TABLE XII
COMPARISON OF OPERATION COST AND EFFICIENCY

Optimization strategy	DG-BD strategy	ARG-BD strategy	RG-BD strategy
Day-ahead operation cost ($)	16696.3	16717.1	16790.7
Real-time adjustment cost ($)	411.2	280.9	243.0
Average total operation cost ($)	17107.5	16998.0	17033.7
Operation time (s)	11.3	22.5	11.5

the highest cost, while the expected real-time adjustment cost is exactly the opposite. The RG-BD strategy achieves the most densely distributed total operation costs and the lowest expected real-time adjustment cost, indicating that under the same WPG scenario, it takes the lowest real-time adjustment cost to deal with the deviation between the actual WPG output and the predicted output, that is, the ability to deal with the uncertainty of WPG is the best. It also can be observed that the ARG-BD strategy is able to effectively deal with the WPG uncertainty and achieves the best economy. This is due to the fact that in the day-ahead stage, the DG-BD model ignores the uncertainties and the RG-BD model puts worst-case scenarios as the highest priority. While the presented ARG-BD model reasonably characterizes the WPG uncertainty by employing the uncertain interval and adjustable robust parameter, which enables the obtained day-ahead ARG-BD strategy to achieve good economy and effectively deal with the WPG uncertainty. Table XII demonstrates that the presented two-stage ARG-BD model takes the longest time to achieve the DA-BD strategy. The solving times of the DG-BD model and the RG-BD model are quite comparable. The reason is that the DG-BD model and the RG-BG model consider the prediction scenario and the worst-case scenario of WPG respectively, and both of them are a single stage model. The presented two-stage ARG-BD model includes the day-ahead stage and real-time stage. The two stages interact with each other. Therefore, the solving efficiency of the presented two-stage ARG-BD model is lower than that of the DG-BD model and the RG-BG model.

VI. Conclusion

This paper presents a blockchain-enabled robust-game electricity transaction model for MMS considering the WPG uncertainty and the specific operation and regulation behaviors of individual microgrids. In this method, game theory is employed to analyze the complicated interest interaction between the individual trading microgrids, and blockchain technology is applied to achieve the effective data management and information interaction in MMS transactions. The distributed MMS transaction architecture constructed by combining blockchain technology and non-cooperative game theory can achieve the decentralized and transparent MMS transaction according to the pre-described energy trading rules. The MMS robust-game model is presented to obtain the optimal DA-BD strategies of MMS, in which the individual microgrid two-stage ARG-BD model characterizes the WPG uncertainty by employing the uncertain interval and adjustable robust parameter. The binary expansion method, duality theory, big M method, and C&CG algorithm are employed to solve the individual microgrid two-stage ARG-BD model. The optimal DA-BD strategies of MMS can be achieved by integrating the C&CG algorithm and non-cooperative game theory, which are able to balance the interests of the microgrid individuals and effectively cope with the WPG uncertainty. The case study indicates that the presented blockchain-enabled robust-game electricity transaction model is able to achieve the transparent and decentralized electricity transaction without intervention of a third trusted party, improves the overall economy of MMS, promotes the WPG consumption, handles the conflict of interest between different trading microgrids and effectively copes with the WPG uncertainty.

References

[1] Q. M. Yang, G. F. Li, Z. H. Bie, J. Y. Wu, C. F. Lin, and D. F. Liu, “Coordinated Power Supply Restoration Method of Resilient Urban Transmission and Distribution Networks Considering Intermittent New Energy,” *High Voltage Engineering*, vol. 49, no. 7, pp. 2764–2774, 2023, doi: 10.13336/j.1003-6520.hve.20230574.

[2] Q. M. Yang, G. F. Li, Z. H. Bie, J. Y. Wu, C. L. Ji, and D. F. Liu, “Vehicle-to-grid Based Resilience Promotion Strategy for Urban Distribution Network Under Typhoon Disaster,” *Automation of Electric Power Systems*, vol. 46, no. 12, pp. 130–139, 2022.

[3] J. Sarshar, S. S. Moosapour, and M. Joorabian, “Multi-objective energy management of a micro-grid considering uncertainty in wind power forecasting,” *Energy*, vol. 139, no. 15, pp. 680–693, Nov. 2017.

[4] Y. Du, Z. W. Wang, G. Y. Liu, X. Chen, H. Y. Yuan, Y. L. Wei, and F. X. Li, “A cooperative game approach for coordinating multi-microgrid operation within distribution systems,” *Applied Energy*, vol. 222, pp. 383–395, Jul. 2018.

[5] R. Aboli, M. Ramezani, and H Falaghi, “A hybrid robust distributed model for short-term operation of multi-microgrid distribution networks,” Electric *Power Systems Research*, vol. 177, pp. 106011, Dec. 2019.

[6] Z. Bo, X. J. Wang, D. Lin, M. M. Calvin, J. C. Morgan, R. W. Qin, and C. S. Wang, “Energy management of multiple microgrids based on a system of systems architecture,” *IEEE Transactions on Power Systems*, vol. 33, no. 6, pp. 6410–6421, Nov. 2018.

[7] A. Jafari, H. G. Ganjehlou, T. Khalili, and A. Bidram, “A fair electricity market strategy for energy management and reliability enhancement of islanded multi-microgrids,” *Applied Energy*, vol. 270, pp. 115170, Jul. 2020.

[8] H Karimi and S. Jadid, “Optimal energy management for multi-microgrid considering demand response programs: A stochastic multi-objective framework,” *Energy*, vol. 195, pp. 116992, Mar. 2020.

[9] Y. C. Jia, P. Wen, Y. S. Yan, and L. M. Huo, “Joint operation and transaction mode of rural multi microgrid and distribution network,” *IEEE Access*, vol. 9, pp. 14409–14421, Jan. 2021, doi: 10.1109/ACCESS.2021.3050793.

[10] J. Mei, C. Chen, J. H. Wang, and J. L. Kirtley, “Coalitional game theory based local power exchange algorithm for networked microgrids,” *Applied Energy*, vol. 239, pp. 133–141, Apr. 2019.

[11] B. Y, Zhang, Q. Q. Li, L. H. Wang, and W. Feng, “Robust optimization for energy transactions in multi-microgrids under uncertainty,” *Applied Energy*, vol. 217, pp. 346–360, May 2018.

[12] Z. M. Li and Y. Xu, “Temporally-coordinated optimal operation of a multi-energy microgrid under diverse uncertainties,” *Applied Energy*, vol. 240, pp. 719–729, Apr. 2019.

[13] Y. X. Liu, L. Guo, and C. S. Wang, “A robust operation-based scheduling optimization for smart distribution networks with multi-microgrids,” *Applied Energy*, vol. 228, pp. 130–140, Oct. 2018.

[14] AH. E. Keshta, A. A. Ali, E. M. Saied, and F. M. Bendary, “Real-time operation of multi-micro-grids using a multi-agent system,” *Energy*, vol. 174, pp. 576–590, May 2019.

[15] M. R. Sandgani and S. Sirouspour, “Coordinated optimal dispatch of energy storage in a network of grid-connected microgrids,” *IEEE Transactions on Sustainable Energy*, vol. 8, no. 3, pp. 1166–1176, Jul. 2017, doi: 10.1109/TSTE.2017.2664666.

[16] B. F. Tan and H. Y. Chen, “Multi-objective energy management of multiple microgrids under random electric vehicle charging,” *Energy*, vol. 208, pp. 118360, Oct. 2020.

[17] R. Z. Jiang, X. Y. Qiu, and D. Li, “Multi-agent system based dynamic game model of smart distribution network containing multi-microgrid,” *Power System Technology*, vol. 38, no. 12, pp. 3321–3327, Dec. 2014.

[18] M. Jalali, K. Zare, and H. Seyedi, “Strategic decision-making of distribution network operator with multi-microgrids considering demand response program,” *Energy*, vol. 141, pp. 1059–1071, Dec. 2017.

[19] M. M. Esfahani, A. Hariri, and O. A. Mohammed, “A multiagent-based game-theoretic and optimization approach for market operation of multimicrogrid systems,” *IEEE Transactions on Industrial Informatics*, vol. 15, no. 1, pp. 280–292, Jan. 2019, doi: 10.1109/TII.2018.2808183.

[20] F. S. Gazijahani and J. Salehi, "Game theory based profit maximization model for microgrid aggregators with presence of EDRP using information gap decision theory," *IEEE Systems Journal*, vol. 13, no. 2, pp. 1767–1775, Jun. 2019, doi: 10.1109/JSYST.2018.2864578.

[21] A. Paudel, K. Chaudhari, C. Long, and H. B. Gooi, "Peer-to-peer energy trading in a Prosumer-based community microgrid: A game-theoretic Model," *IEEE Transactions on Industrial Electronics*, vol. 66, no. 8, pp. 6087–6097, Aug. 2019, doi: 10.1109/TIE.2018.2874578.

[22] G. Q. Li, R. F. Zhang, T. Jiang, H. H. Chen, L. Q. Bai, and X. J. Li, "Security-constrained bi-level economic dispatch model for integrated natural gas and electricity systems considering wind power and power-to-gas process," *Applied Energy*, vol. 194, pp. 696–704, May 2017.

[23] H. F. Qiu and F. Q. You, "Decentralized-distributed robust electric power scheduling for multi-microgrid systems," *Applied Energy*, vol. 269, pp. 115146, Jul. 2020.

[24] T. G. Lu, Q. Ai, and Z. Y. Wang, "Interactive game vector: A stochastic operation-based pricing mechanism for smart energy systems with coupled-microgrids," *Applied Energy*, vol. 212, pp. 1462–1475, Feb. 2018.

[25] H. F. Qiu, W. Gu, Y. L. Xu, Z. Wu, S. Y. Zhou, and G. S. Pan, "Robustly multi-microgrid scheduling: stakeholder-parallelizing distributed optimization," *IEEE Transactions on Sustainable Energy*, vol. 11, pp. 2, pp. 988–1001, Apr. 2020.

[26] H. F. Qiu, B. Zhao, W. Gu, and R. Bo, "Bi-level two-stage robust optimal scheduling for AC/DC hybrid multi-microgrids," *IEEE Transactions on Smart Grid*, vol. 9, no. 5, pp. 5455–5466, Sep. 2018, doi: 10.1109/TSG.2018.2806973.

[27] M. H. Shams, M. Shahabi, M. Mansourlakouraj, M. Shafie-Khah, and J. P. S. Catalão, "Adjustable robust optimization approach for two-stage operation of energy hub-based microgrids," *Energy*, vol. 222, pp. 119894, May 2021.

[28] C. Wang, W. Wei, J. H. Wang, and T. S. Bi, "Convex optimization based adjustable robust dispatch for integrated electric-gas systems considering gas delivery priority," *Applied Energy*, vol. 239, pp. 70–82, Apr. 2019.

[29] M. H. Shams, M. Shahabi, M. Mansourlakouraj, M. Shafie-Khah, and J. P. S. Catalão, "Adjustable robust optimization approach for two-stage operation of energy hub-based microgrids," *Energy*, vol. 222, pp. 119894, May 2021.

[30] X. C. Li, Y. X. Liu, G. Li, X. L. Li, and C. S. Wang, "Data-driven Based Uncertainty Set Modeling Method for Microgrid Robust Optimization with Correlated Wind Power," *Proceedings of the CSEE*, vol. 9, no. 2, pp. 420–432, 2023.

[31] Y. Liu, X. B. Chen, L. Wu, and Y. L. Ye, "Distributionally Robust Economic Dispatch Using IDM for Integrated Electricity-heat-gas Microgrid Considering Wind Power," *Proceedings of the CSEE*, vol. 9, no. 3, pp. 1182–1192, 2023.

[32] N. Z. Aitzhan and D. Svetinovic, "Security and privacy in decentralized energy trading through multi-signatures, blockchain and anonymous messaging streams," *IEEE Transactions on Dependable and Secure Computing*, vol. 15, no. 5, pp. 840–852, Sep./Oct. 2018, doi: 10.1109/TDSC.2016.2616861.

[33] W. Tushar, T. K. Saha, C. Yuen, T. Morstyn, Nahid-Al-masood, H. V. Poor, and R. Bean, "Grid influenced peer-to-peer energy trading," *IEEE Transactions on Smart Grid*, vol. 11, no. 2, pp. 1407–1418, Mar. 2020, doi: 10.1109/TSG.2019.2937981.

[34] D. C. Yang, X. Y. Zhao, Z. X. Xu, Y. Li, and Q. Li, "Developing status and prospect analysis of blockchain in energy internet," *Proceedings of the CSEE*, vol. 37, no. 13, pp. 3664–3671, Jul. 2017.

[35] F. J. Luo, Z. Y. Dong, G. Q. Liang, J. Murata, and Z. Xu, "A distributed electricity trading system in active distribution networks based on multi-agent coalition and blockchain," *IEEE Transactions on Power Systems*, vol. 34, no. 5, pp. 4097–4108, Sep. 2019.

[36] G. J. Gong, H. J. Wang, T. Zhang, Z. M. Chen, P. F. Wei, C. Su, Y. F. Wen, and X. J. Xiang, "Research on Electricity Market About Spot Trading Based on Blockchain," *Proceedings of the CSEE*, vol. 38, no. 23, pp. 6955–6966, Dec. 2018.

[37] T. M. Masaud, J. Warner, and E. F. El-Saadany, "A blockchain-enabled decentralized energy trading mechanism for islanded networked microgrids," *IEEE Access*, vol. 8, pp. 211291–211302, Nov. 2020, doi: 10.1109/ACCESS.2020.3038824.

[38] Y. N. Jiang, K. L. Zhou, X. H. Lu, and S. L. Yang, "Electricity trading pricing among prosumers with game theory-based model in energy blockchain environment," *Applied Energy*, vol. 271, pp. 115239, Aug. 2020.

[39] B. Y. Liu, M. Wang, J. Men, and D. C. Yang, "Microgrid trading game model based on blockchain technology and optimized particle swarm algorithm," *IEEE Access*, vol. 8, pp. 225602–225612, Dec. 2020, doi: 10.1109/ACCESS.2020.3044980.

[40] F. S. Gazijahani and J. Salehi, "Game theory based profit maximization model for microgrid aggregators with presence of EDRP using information gap decision theory," *IEEE Systems Journal*, vol. 13, no. 2, pp. 1767–1775, Jun. 2019, doi: 10.1109/JSYST.2018.2864578.

[41] G. Van Leeuwen, T. Alskaif, M. Gibescu, and W. Van Sark, "An integrated blockchain-based energy management platform with bilateral trading for microgrid communities," *Applied Energy*, vol. 263, pp. 114613, Apr. 2020.

[42] M. L. Di Silvestre, P. Gallo, M. G. Ippolito, R. Musca, E. R. Sanseverino, Q. T. T. Tran, and G. Zizzo, "Ancillary services in the energy blockchain for microgrids," *IEEE Transactions on Industry Applications*, vol. 55, no. 6, pp. 7310–7319, Nov./Dec. 2019.

[43] M. T. Devine and P. Cuffe, "Blockchain electricity trading under demurrage," *IEEE Transactions on Smart Grid*, vol. 10, no. 2, pp. 2323–2325, Mar. 2019, doi: 10.1109/TSG.2019.2892554.

[44] J. Y. Wu, Y. Liu, X. B. Chen, C. H. Wang, and W. F. Li, "Data-driven adjustable robust Day-ahead economic dispatch strategy considering uncertainties of wind power generation and electric vehicles," *International Journal of Electrical Power & Energy Systems*, vol. 138, pp. 107898, Jun. 2022.

Jiayu Wu received B.S. and M.S. degrees in Electrical Engineering from Sichuan University, Chengdu, China, in 2019 and 2022, respectively. Her research interests include distribution network planning and operations, and application of blockchain technology in electricity transactions.

Yang Liu received a B.S. degree in Electrical Engineering from Sichuan University, Chengdu, China, in 2005, and M.Sc. and Ph.D. degrees from the School of Engineering and Design, Brunel University, Uxbridge, U.K., in 2006 and 2011, respectively. He is currently an Associate Professor in the College of Electrical Engineering, Sichuan University. His research interests include microgrid planning and operations, unit commitment, economic dispatch, and electricity data analysis.

Qiming Yang received a B.S. degree in Electrical Engineering from Sichuan University, Chengdu, China, in 2021. He is currently working toward an M.S. degree in Electrical Engineering from Xi'an Jiaotong University, Xi'an, China. His research interests include power system resilience and electrical vehicle dispatch strategy.

Wenfeng Li received B.S. and Ph.D. degrees in Electrical Engineering from Sichuan University, Chengdu, China, in 2008 and 2013, respectively. His research interests include distribution network planning and operationa, and electricity data analysis.